Nanoscale

PAPER

View Article Online
View Journal | View Issue

Cite this: *Nanoscale*, 2017, **9**, 5489

Activation of autophagy by elevated reactive oxygen species rather than released silver ions promotes cytotoxicity of polyvinylpyrrolidone-coated silver nanoparticles in hematopoietic cells

Lingying Zhu,†[a] Dawei Guo,†[b] Lili Sun,[c] Zhihai Huang,[a] Xiuyan Zhang,[d] Wenjuan Ma,[d] Jie Wu,[d] Lun Xiao,[d] Yun Zhao[d] and Ning Gu *[a,e]

Received 19th October 2016,
Accepted 22nd March 2017

DOI: 10.1039/c6nr08188f

rsc.li/nanoscale

Silver nanoparticles (AgNPs) are the most commonly used engineered nanomaterials in commercialized products because of their antimicrobial activity. Previously, we have shown that polyvinylpyrrolidone (PVP)-coated AgNPs have an anti-leukemia effect against human myeloid leukemia cells; however, whether AgNPs are able to trigger autophagy in normal hematopoietic cells and the role of autophagy in AgNP-induced cytotoxicity remain unclear. In the current study, we observed that AgNPs were taken up by murine pro-B cells (Ba/F3), and then promoted accumulation of autophagosomes, which resulted from the induction of autophagy rather than the blockade of autophagic flux. AgNPs induced cytotoxicity in a dose-dependent manner accompanied by apoptosis and DNA damage through the production of reactive oxygen species (ROS) and the release of silver ions. The ROS-mediated mTOR signaling pathway was responsible for the induction of autophagy. More importantly, the inhibition of autophagy with the addition of 3-methyladenine (3-MA) or silencing of *Atg5* significantly attenuated the cytotoxicity of AgNPs in Ba/F3. These findings suggest that autophagy is involved in the cytotoxicity of PVP-coated AgNPs in normal hematopoietic cells, and the inhibition of autophagy is a novel and potent strategy to protect normal hematopoietic cells upon treatment with AgNPs.

Introduction

Silver nanoparticles (AgNPs) have become the most widely commercialized nanomaterials due to their well-known antibacterial properties.[1,2] Inevitably, the growing applications have increased the possibility of human exposure to AgNPs through inhalation, ingestion, injection for therapeutic purpose and dermal contact. Once inside the body, AgNPs are distributed throughout the main organs, especially in the kidney, liver, spleen and brain *via* blood circulation.[3–5] Therefore, more studies are needed to focus on the effects of AgNPs on normal blood cells. A 28-day repeated dose toxicity study in rats has shown that AgNP accumulation is noted in the spleen, liver and lymph nodes; in addition, a severe increase in spleen size and weight is shown due to the increased number of both T and B cells.[6] Therefore, in this study we chose the murine bone marrow pro-B cell, Ba/F3, as a cell model, which has been used to investigate the crosstalk between autophagy and apoptosis.[7] Bone marrow pro-B cells are differentiated and developed into mature B cells located in the spleen and lymph nodes, associated with a series of immune responses. Furthermore, we have performed some fundamental studies on the effect of AgNPs on BCR/ABL expressed Ba/F3 cells independent of murine interleukin-3 (mIL-3),[8] which will be of great importance to further investigate the effect of AgNPs on normal Ba/F3 cells.

An increasing number of studies have demonstrated that AgNPs have toxic effects on various cells and organisms,[9,10] which becomes a potential threat to the health of human beings or possibly is helpful in the combat against diseases. The mechanism underlying the cytotoxicity of AgNPs, however, is yet to be fully addressed. It is well established that the exposure of AgNPs is sufficient to enhance the generation of reactive oxygen species (ROS), which is responsible for the

[a]*State Key Laboratory of Bioelectronics, Jiangsu Key Laboratory for Biomaterials and Devices, School of Biological Science and Medical Engineering, Southeast University, Nanjing 210096, PR China. E-mail: guning@seu.edu.cn*
[b]*Laboratory of Veterinary Pharmacology and Toxicology, College of Veterinary Medicine, Nanjing Agricultural University, Nanjing 210095, PR China*
[c]*The Experimental Center, The Second Affiliated Hospital of Soochow University, Suzhou 215123, PR China*
[d]*Collaborative Innovation Center of Hematology, Soochow University, Suzhou 215006, PR China*
[e]*Collaborative Innovation Center of Suzhou Nano-Science and Technology, Suzhou Key Laboratory of Biomaterials and Technologies, Suzhou 215123, PR China*
†These authors contributed equally to the manuscript.

AgNP-induced cytotoxicity,[11] and is also the key regulator of autophagy.[12] The physiological levels of ROS lead to growth adaption and survival while excessive ROS causes irreversible cellular damage, thus provoking autophagy or apoptosis.[13] Autophagy and lysosomal dysfunction have been considered as an emerging toxic mechanism of nanomaterials.[14] Autophagy is a programmed cell death process besides apoptosis,[15] and acts as either a cellular survival or death mechanism depending on different environmental stresses and cell types.[16,17] Accumulating data have demonstrated that nanomaterials including AgNPs trigger cellular autophagy.[18–22] In addition, we are able to show that AgNPs induce autophagy in some cancer cells.[23–25] However, whether AgNPs are able to induce autophagy in normal hematopoietic cells remains unclear. Previously, we have shown that PVP-coated AgNPs exert their cytotoxic effect against leukemic cells partially *via* the generation of ROS,[26,27] an effective inducer of autophagy, and thus it's reasonable to speculate that autophagy is triggered by PVP-coated AgNPs. Autophagy plays a paradoxical role in AgNP-induced cytotoxicity. On the one hand, elevated autophagy upon AgNP treatment leads to increased cell death.[28] On the other hand, AgNP-induced autophagy promotes cell survival as demonstrated in our previous results.[24] A detailed mechanism of cell-specific cytotoxicity of AgNPs will contribute to their application. Thus it is of importance to delineate the role of speculated autophagy induced by AgNPs in normal blood cells.

In the present study, we investigated the effects of well-characterized PVP-coated AgNPs on an immortalized murine pro-B cell (Ba/F3). Our data clearly showed that the treatment with AgNPs led to autophagy through the PI3K-mTOR signaling pathway along with the well-established cytotoxicity caused by both generation of ROS and release of silver ions. Interestingly, only ROS was responsible for the induction of autophagy. Lastly, autophagy contributed to apoptosis and DNA damage induced by AgNPs. Taken together, these data have deepened the understanding of the cytotoxic mechanisms of AgNPs, which would shed light on how to utilize these nanoparticles properly.

Results and discussion

Characterization of silver nanoparticles

Transmission electron microscopy (TEM) was used to observe the particle morphology of the as-synthesized silver nanoparticles (AgNPs). As depicted in Fig. 1A, the typical morphology of AgNPs had an approximate spherical shape without any agglomeration. The uniform AgNPs had an average diameter of 11.17 ± 0.62 nm ranging from 8 to 14 nm (Fig. 1B). In the current study, polyvinylpyrrolidone (PVP, K30) was employed as a stabilizing agent due to its attachment onto the AgNPs' surface *via* the carbonyl group.[29] In addition, protein adsorption in the culture media supplemented with serum improved the stability of PVP-coated AgNPs due to the enhanced steric hindrance.[27,30] Once inside the Ba/F3 cells,

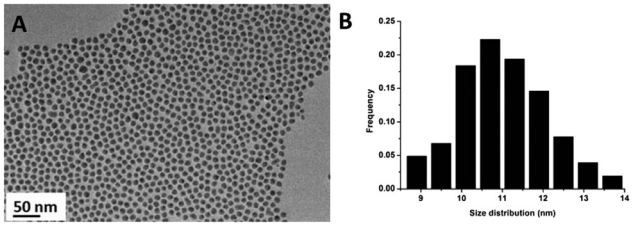

Fig. 1 Characterization of silver nanoparticles (AgNPs). (A) The morphology of AgNPs was characterized by transmission electron microscopy (TEM). (B) The size distribution histograms were obtained by size analysis of over 200 particles.

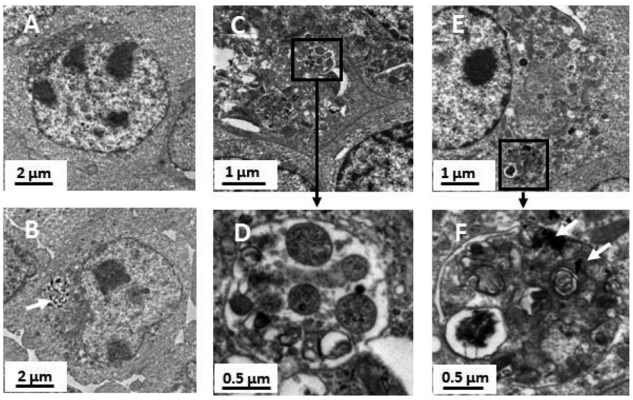

Fig. 2 TEM images of Ba/F3 cells incubated for 24 h without (A) or with 8 μg mL^{-1} AgNPs (B–F). Inset: Close-up of the enlarged lysosomes (scale bar, 0.5 μm). AgNPs were internalized by cells and trapped inside lysosomes (white arrow).

AgNPs were inclined to form aggregates (Fig. 2B). PVP-stabilized AgNPs entered the cells *via* endocytosis, as uptake could be prevented by an endocytosis inhibitor.[31] Therefore, we found that AgNPs were mainly located in the lysosomes of Ba/F3 cells (Fig. 2B). The intracellular concentrations of AgNPs could be reflected by the intensity of side scatter light detected by flow cytometry, which increased in a dose-dependent manner compared to the control cells (Fig. 3A), while the side-scatter intensity of cells exposed to silver ions was not altered (Fig. 3B). The Ba/F3 cells incubated with AgNPs at 4 °C and 37 °C exhibited different side-scattering intensities (Fig. 3C), indicating that the uptake of AgNPs was partially energy dependent. To quantitatively analyze the cellular uptake of AgNPs, inductively coupled plasma mass spectrometry (ICP-MS) measurements were performed to estimate the amount of silver internalized by Ba/F3 cells exposed to AgNPs (8 μg mL^{-1}). About 20% of the total amount of silver inside the cells was present in the ionic form and the remaining was present in nanoparticles (Fig. 3D). However, silver ions were not detected by ICP-MS in the de-ionized water and RPMI-1640 medium with the same concentration of AgNPs, suggesting that the detected silver ions inside the AgNP-treated cells were released from AgNPs after their internalization into cells, which was in agreement with our previous study.[26,32]

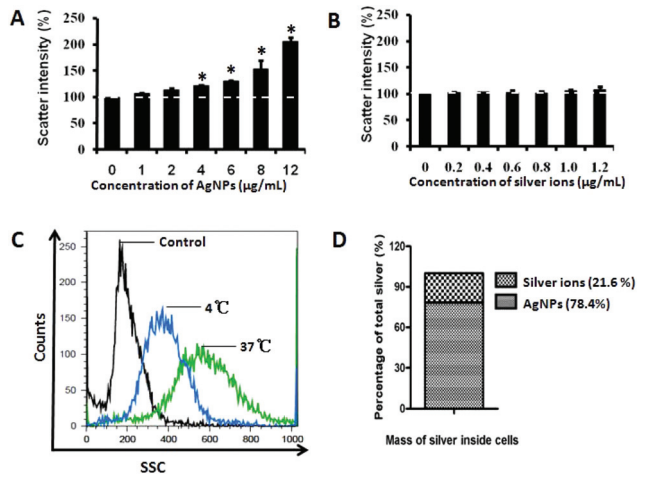

Fig. 3 Intracellular occurrence of AgNPs in Ba/F3 cells analyzed by flow cytometric light-scattering analysis (A–C) and ICP-MS (D). (A) Dose-dependent scattering intensities as a percentage of control for Ba/F3 cells treated with AgNPs (A) or silver ions (B) for 4 h. (C) The cells were incubated at 4 °C and 37 °C in the presence of AgNPs (12 μg mL^{-1}). (D) The proportion of AgNPs and Ag^+ inside Ba/F3 cells upon 24 h AgNPs (8 μg mL^{-1}) treatment is shown. Mean ± SD, n = 3. *P < 0.05.

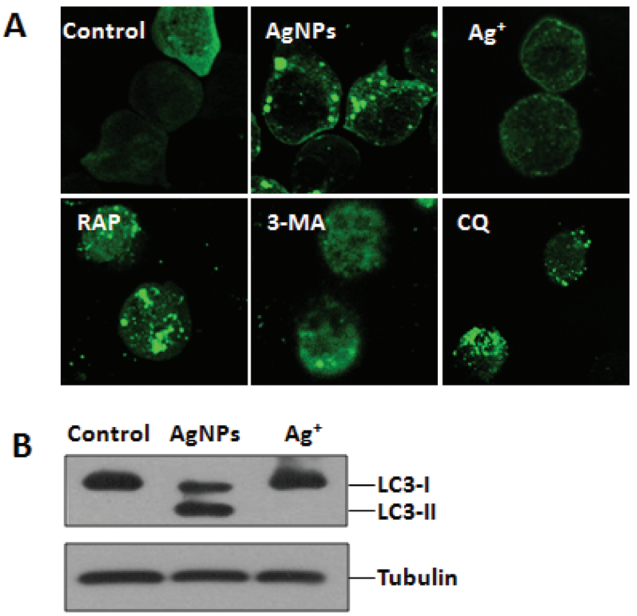

Fig. 4 Induction of autophagy by AgNPs treatment. (A) Fluorescent microscopy images of GFP-LC3-Ba/F3 cells treated with PBS (control), 8 μg mL^{-1} AgNPs, 1 μg mL^{-1} silver ions, 500 ng mL^{-1} RAP, 2 μM 3-MA and 2 μM CQ alone for 24 h. (B) The level of LC3-II was detected by western blot in Ba/F3 cells treated with AgNPs or silver ions for 24 h.

AgNPs triggered autolysosomes accumulation

Once engulfed by cells, the subsequent fate of AgNPs has aroused much interest. Many inorganic nanoparticles cannot be degraded in the living cells,[14,33] thus the autophagic process may be the only self-clearance way. Autophagy has been reported to play a vital role in modulating many important physiological functions such as cell survival and death.[16,17] In the present study, TEM analysis confirmed that the AgNPs induced the accumulation of autophagosomes in Ba/F3 cells (Fig. 2C and E), and cytosolic autophagosomes and vacuolization were clearly visualized in the images with higher magnification (Fig. 2D and F). The formation of autophagosomes involves complex protein pathways, one of which includes the conjugation of an ubiquitin-like protein, microtubule-associated protein 1 light chain 3 (LC3).[34] It is cleaved at the C-terminal to release a cytosolic form LC3-I, and then covalently conjugated to the lipid phosphatidylethanolamine (PE) to yield LC3-II (an important protein marker for autophagic activity), which is further translocated into the mature autophagosome membrane.[35] Accordingly, Ba/F3 cells were transfected with GFP-LC3-II. The confocal analysis showed that the AgNP-treated cells similar to RAP-stimulated cells displayed more GFP-LC3-II puncta than the control cells (Fig. 4A). In addition, western blotting further confirmed that LC3-II increased upon AgNP treatment compared with the control cells (Fig. 4B). Collectively, these pieces of evidence strongly supported that AgNPs induced autophagy in Ba/F3 cells. However, it is interesting to note that silver ions did not induce the up-regulation of LC3-II (Fig. 4A and B), indicating that silver ions were not able to induce autophagy in Ba/F3 cells.

AgNPs enhanced autophagic activity but not decreased autophagosome formation turnover

LC3-II could be degraded in autolysosomes, so the total amount of LC3-II is determined by the balance between production and degradation. However, when lysosomal degradation is inhibited, the amount of LC3-II is strictly dependent on its production. Therefore, we can ascertain whether or not autophagosome accumulation results from either true induction of autophagy activity or blockade of autophagic flux by comparing the amount of LC3-II in the presence and absence of an autolysosome degradation inhibitor.[36] To distinguish these two possibilities, Ba/F3 cells were treated with AgNPs plus chloroquine (CQ), which prevents degradation of the autolysosome content by inhibiting vacuolar H^+ ATPase activity as an autophagy inhibitor. AgNP-induced enhancement of LC3-II formation was further increased by the addition of CQ (Fig. 5B), which indicated that autophagic turnover was not impaired by treatment with AgNPs. To shed more light on this conclusion, the autophagic degradation was monitored by measuring the expression of p62 (also known as SQSTM1/sequestome1, a substrate preferentially degraded by autolysosomes),[37] which was decreased upon exposure to AgNPs (Fig. 5A). Taken together, these results showed that accumulation of autophagosomes caused by AgNPs resulted from increased autophagic activity rather than decreased autophagic turnover.

Particles often end up in lysosomes with a lower pH (around pH 5.5) that can enhance the rate of dissolution of some particles.[38,39] The participation of lysosomes in auto-

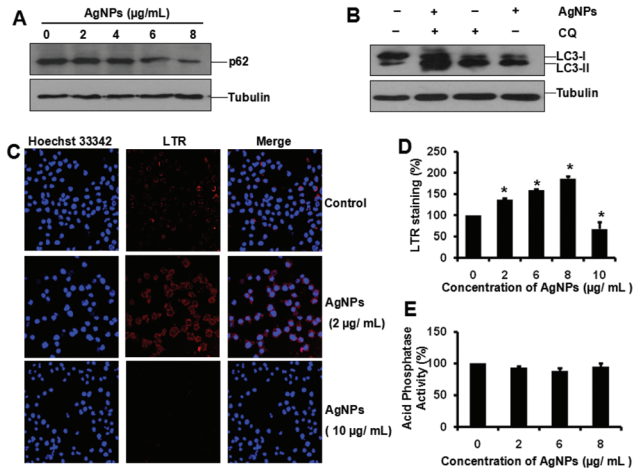

Fig. 5 Effect of AgNPs on autophagic flux and lysosome dysfunction. (A) Western blot of p62 in Ba/F3 cells treated with various concentrations of AgNPs for 24 h. β-Tubulin served as loading control. (B) Western blot of LC3 in Ba/F3 cells treated with AgNPs (8 μg mL^{-1}) for 24 h in the presence or absence of 2 μM CQ. (C) Fluorescent microscopy images and (D) FACS analysis of Ba/F3 cells treated with AgNPs (0–10 μg mL^{-1}) for 24 h. Cells were exposed to 1 μM LysoTracker Red DND-189 for 30 min. (E) Acid phosphatase enzyme activity of Ba/F3 cells was measured after the cells were treated with AgNPs for 24 h. Mean ± SD, $n = 3$. *$P < 0.05$.

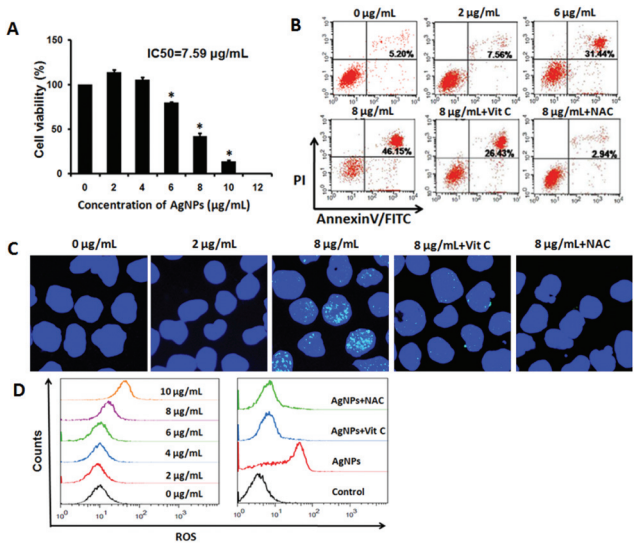

Fig. 6 Cytotoxicity of Ba/F3 cells induced by AgNPs. (A) Effect of AgNPs (0–12 μg mL^{-1}) on the viability of Ba/F3 cells detected by CCK-8 assay. (B) Effect of AgNPs (8 μg mL^{-1}) on apoptosis in the presence or absence of Vit C or NAC for 24 h. (C) Confocal images of DNA damage induced by AgNPs in the presence or absence of Vit C or NAC measured using the expression of γ-H2AX. (D) Effect of AgNPs on the production of ROS. Generation of ROS in Ba/F3 cells exposed to AgNPs at various concentrations (0–10 μg mL^{-1}) (left). Cells were treated with AgNPs (8 μg mL^{-1}) in the presence or absence of Vit C or NAC for 3 h (right).

phagy was further confirmed by the analysis of lysosomal activation using LysoTracker Red (LTR). The data showed that treatment with AgNPs (2–8 μg mL^{-1}) caused enhancement in both volume and frequency of cytoplasmic granules staining with LTR, quite different from the treatment with AgNPs at a higher concentration (10 μg mL^{-1}) (Fig. 5C and D), and the activity of acid phosphatase, a kind of lysosome marker enzyme, was not significantly affected after exposure to AgNPs (0–8 μg mL^{-1}) (Fig. 5E), indicating that the lysosome degradation capacity was not destroyed by exposure to AgNPs, in line with the autophagic flux assay results described above.

AgNPs induced autophagy in a ROS-dependent manner

A significant increase of the ROS level was detected compared with the untreated cells, which could be effectively inhibited by the antioxidants vitamin C (Vit C, 50 μM) and *N*-acetylcysteine (NAC, 5 mM) (Fig. 6D). Both Vit C and NAC were also capable of protecting cells from apoptosis and DNA damage induced by AgNPs (Fig. 6B and C), suggesting that the generation of ROS contributed to apoptosis and DNA damage induced by AgNPs in Ba/F3 cells. However, NAC could totally rescue while Vit C partially rescued the AgNP-induced apoptosis and DNA damage (Fig. 6B and C), which was in line with others' data.[40] Besides working as an antioxidant, NAC also served as a silver ion chelator.[41] Therefore, these results suggested that oxidative stress together with ionic silver release mediated cytotoxicity of AgNPs in Ba/F3 cells.

It has also been reported that ROS accumulation could regulate autophagy in various cells.[42–44] Therefore, further investigation was performed to study whether ROS scavenging could inhibit AgNP-promoted autophagy. The pretreatment with Vit C and NAC significantly decreased the number of monodansylcadaverine (MDC) positive autophagic vacuoles (Fig. 7A) and the intensity of LTR staining (Fig. 7B). Most of the investigated nanoparticles inhibited mTOR activation in various normal and malignant cells,[45] which led to cell dysfunction and death, accompanied by an increased autophagic response.[46–48] In the present study, the levels of phosphory-

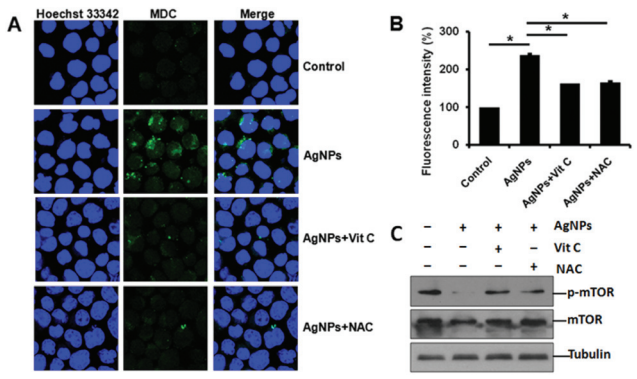

Fig. 7 ROS production mediates autophagy induced by AgNPs in a mTOR-dependent manner. Effect of the ROS scavengers Vit C and NAC on the reduction in cell autophagy induced by AgNPs detected by MDC staining (A) and LysoTracker Red assay (B). (C) Cells exposed to AgNPs for 24 h in the presence or absence of Vit C or NAC were analyzed for mTOR activity by protein gel blotting for the levels of total (mTOR) and phosphor mTOR (p-mTOR). Mean ± SD, $n = 3$. *$P < 0.05$.

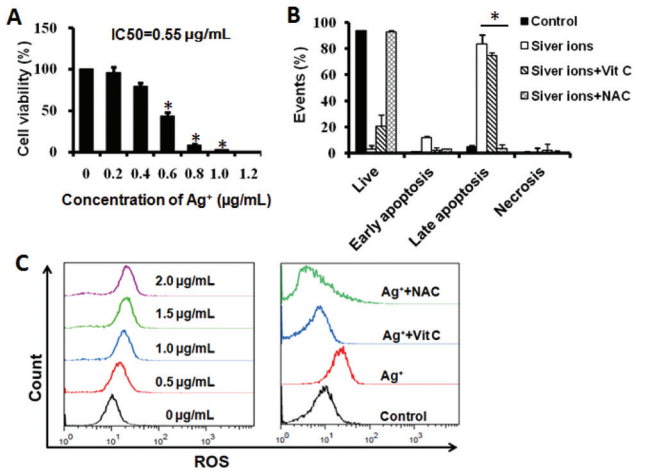

Fig. 8 Cytotoxic effect of Ba/F3 cells induced by silver ions. (A) Effect of silver ions (0–1.2 μg mL^{-1}) on the viability of Ba/F3 cells detected by CCK-8 assay. (B) Cellular apoptosis of various silver ion-treated cells was detected by Annexin V/PI staining. (C) Effect of silver ions on production of ROS. Generation of ROS in Ba/F3 cells exposed to silver ions at various concentrations (0–2.0 μg mL^{-1}) (left). Cells were treated with silver ions (1.0 μg mL^{-1}) in the presence or absence of Vit C or NAC for 3 h (right).

lated mTOR were inhibited by AgNPs, and then restored by treatment with Vit C and NAC (Fig. 7C), which indicated that the ROS-mediated mTOR signaling pathway was possibly responsible for the autophagy induced by AgNPs. Silver ions exhibited much stronger cytotoxicity than PVP-coated AgNPs (Fig. 6A and 8A), and AgNPs and silver ions induced ROS at a similar level (Fig. 6D and 8C). Both Vit C and NAC completely suppressed ROS generation (Fig. 8C), however apoptosis induced by the silver ions was not sharply reduced by Vit C, while NAC completely prevented silver ion-induced apoptosis (Fig. 8B), suggesting that silver ions had a special cytotoxic mechanism independent of ROS.[26] Furthermore, exposure to silver ions did not induce autophagy in Ba/F3 cells (Fig. 4A and B). These results indicated that silver ions were not involved in autophagy caused by AgNPs.

Inhibition of autophagy decreased cytotoxicity induced by AgNPs

It has been reported that autophagy can contribute to cell death by selectively removing survival factors and cellular components. There are many publications indicating that autophagy induced by NPs plays an important role in cytotoxicity.[46–48] To determine whether autophagy was involved in AgNP-induced cell death, 3-MA (a kind of autophagy inhibitor),[49] was used to treat Ba/F3 cells with or without AgNPs. After treatment with 3-MA, the apoptosis level of AgNP-treated cells significantly decreased (Fig. 9A). Moreover, pretreatment with 3-MA partially reduced DNA damage induced by AgNPs (Fig. 9B), which indicated that the autophagic pathway plays a role in the cytotoxicity induced by AgNPs. Apoptosis and autophagy are highly interconnected,[50] and many reports have demonstrated that autophagy contributes to cell death.[51] To gain further proof for the role of autophagy in AgNP-elicited cell death, we assessed the function of *Atg5*, an autophagy-

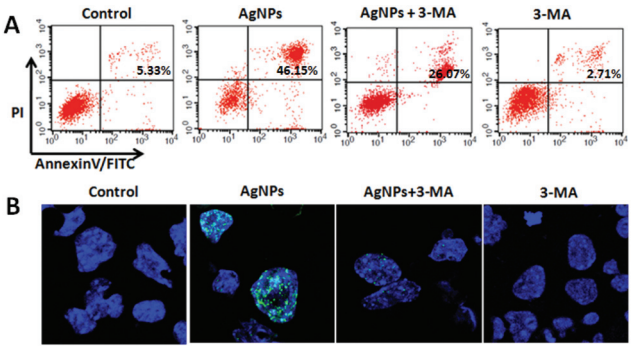

Fig. 9 Inhibition of autophagy through 3-MA prevented apoptosis and DNA damage. (A) The representative images of apoptosis detected by Annexin-V/PI staining are displayed using treatment with AgNPs (8 μg mL^{-1}) in the presence or absence of 3-MA (2 mM). (B) Confocal images of DNA damage (indicated as the expression of γ-H2AX, green) induced by AgNPs (8 μg mL^{-1}) in the presence or absence of 3-MA (2 mM) is shown.

essential gene,[52] in this process. Transfection with Atg5-specific siRNA (shAtg5) led to an effective knockdown of Atg5 protein expression (Fig. 10A). Compared to cells transfected with the negative control siRNA (shNC), Ba/F3 cells transfected with shAtg5 exhibited a significantly increased cell viability (Fig. 10B), but a significantly decreased apoptosis (Fig. 10C) compared with the control cells, and a significant decrease in apoptotic and necrotic cells (Fig. 10C) as measured by the Annex V-FITC/PI assay after AgNPs treatment. Taken together, the above results demonstrated that the autophagy induced by AgNPs played a cytotoxic role on the cell fate, and inhibition of autophagy by either the chemical inhibitor or Atg5 knockdown reduced cytotoxicity of AgNPs in mouse pro-B cells. Autophagy activation has been considered to be a key player in cytotoxicity induced by citrate-AgNPs in mouse

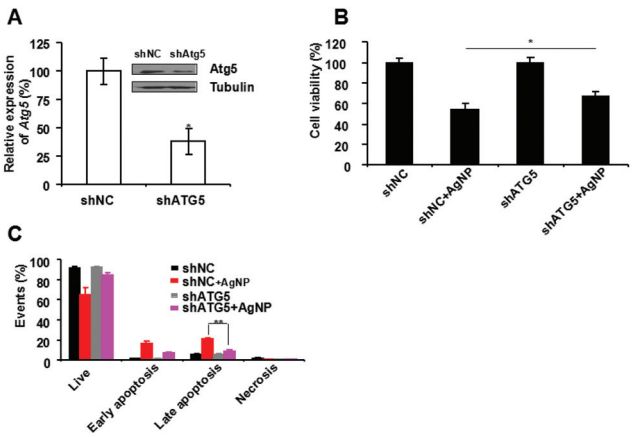

Fig. 10 Inhibition of autophagy by Atg5 siRNA (shAtg5) treatment decreased cytotoxicity of AgNPs in Ba/F3 cells. (A) Western blot of Atg5 in Ba/F3 cells transfected with shAtg5 or control siRNA (shNC) for 24 h. (B) Cell viability of Ba/F3 cells treated with 8 μg mL^{-1} AgNPs for 24 h after transfection with shAtg5 or shNC. (C) Apoptosis of Ba/F3 cells by treatment with 8 μg mL^{-1} AgNPs for 24 h after transfection with shAtg5 or shNC.

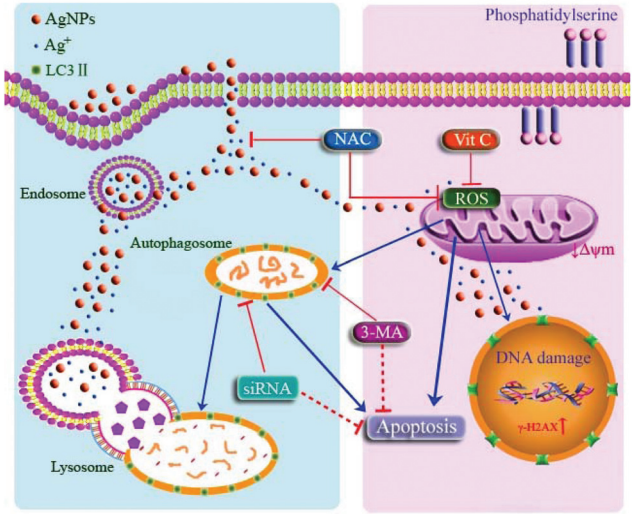

Scheme 1 Schematic presentation of the mechanism underlying AgNP-induced autophagy and its cytotoxic effect in Ba/F3 cells.

embryonic fibroblasts.[28] Autophagosomes accumulation mediates the impedance of PMA-induced monocyte–macrophage differentiation by AgNP treatment in human blood immune cells.[20] Additionally, autophagy can be induced by rare earth upconversion nanoparticles (UCNs) and is detrimental to Kupffer cells. Inhibition of autophagy by 3-MA promotes Kupffer cells survival and abrogates the nanohepatotoxicity.[53] In contrast, our previous report showed that different from the results of these studies, autophagy induced by AgNPs played a protective role in the cancerous U251 cells and HeLa cells.[23,24] In addition, nano-sized paramontroseite VO_2 nanocrystals induce cyto-protective autophagy in cultured HeLa cells.[17] These studies strongly suggest a cell-context dependent role of autophagy in AgNP-induced cytotoxicity.

Conclusion

In this study, we demonstrated that the PVP-coated AgNPs induced autophagy in Ba/F3 cells *via* a ROS-mediated mTOR signaling pathway whereas silver ions did not. Inhibition of autophagy by both a chemical inhibitor and Atg5 silencing significantly attenuated the cytotoxicity of AgNPs in Ba/F3 cells (Scheme 1), suggesting that autophagy induced by the AgNPs promoted the cytotoxic effect of these nanoparticles in Ba/F3 cells. Altogether, these findings provide a novel approach for decreasing the cytotoxic effect of AgNPs on the normal cells in the application of tumor therapy.

Materials and methods

Synthesis and characterization of silver nanoparticles

Silver nanoparticles (AgNPs) were synthesized by a continuous flow electrochemical process. Polyvinylpyrrolidone (PVP, K30) and two silver rods were utilized as stabilizing agents and electrodes, respectively. The electrolytic solution containing 5 mg mL^{-1} PVP was filled into a syringe, and then continuously injected into the reactor. During the reaction, the electrolytic solution was stirred with a magnetic rotor at 60 °C. After the reactor was filled, the product flowed out of the outlet tube of the reactor's cover. Finally, the freeze-dried powders of the AgNPs were obtained after filtration, centrifugation and lyophilization. The morphology of the AgNPs was characterized by transmission electron microscopy (TEM, JEM-2000EX, JEOL, Japan), and over 200 particles from a random field of TEM images were counted and measured to determine the mean size and size distribution. The final silver concentration in all dispersions was determined by inductively coupled plasma mass spectrometry (ICP-MS) using an Optima 5300DV (PerkinElmer, USA).

Cell culture

Ba/F3 cells (an immortalized murine bone marrow-derived pro-B cell line) were suspension cells, which were cultured in RPMI-1640 medium (Hyclone, USA) supplemented with 10% fetal bovine serum (FBS, Hyclone) and 5 ng mL^{-1} murine interleukin 3 (mIL-3, Sigma, St Louis, MO, USA) at 37 °C under a humidified atmosphere of 5% CO_2. All experiments were conducted after 24 h treatment with AgNPs or silver ions.

Transmission electron microscopy (TEM) observation of AgNP-treated cells

Ba/F3 cells (5×10^5 mL^{-1}) were treated with the AgNPs (8 μg mL^{-1}), and then fixed with 2.5% glutaraldehyde, followed by post-fixation with 1% osmium tetroxide (Agar Scientific, Stansted, UK) for 1.5 h. The samples were dehydrated with a graded ethanol series, and then incubated with propylene oxide and araldite resin (1 : 1) overnight. Cell pellets were subsequently embedded in araldite resin at 60 °C for 48 h and ultra-thin sections were made using an ultra microtome (LEICA EM UC6, Netherlands). The sections were mounted onto copper grids and images were captured with a TEM (JEM-2000EX).

Cellular uptake of AgNPs measured by flow cytometry

Ba/F3 cells (5×10^5 mL^{-1}) were incubated at 4 °C or 37 °C in the presence of AgNPs (0–12 μg mL^{-1}) for 24 h. The AgNPs were dispersed in sterile deionized water at a concentration of 135 μg mL^{-1} as a stock solution. Subsequently, the cells were centrifuged and suspended in phosphate buffered saline (PBS), then transferred to 5 mL tubes, and the uptake of particles by the cells was analyzed using flow cytometry (side scattering signal, Calibur™, Becton Dickinson, USA).

Analysis of AgNPs and silver ions inside Ba/F3 cells

Cells (5×10^5 mL^{-1}) were exposed to the AgNPs (8 μg mL^{-1}) for 24 h and then washed with PBS to remove excess particles or those adhered to the cells. Triton-X 114-based cloud point extraction (CPE) was used to separate AgNPs and silver ions in the lysates of Ba/F3 cells after exposure to AgNPs. Cell lysates

were subjected to CPE after adding $Na_2S_2O_3$, which facilitated the transfer of AgNPs into the nether Triton X-114-rich phase by the salt effect and preserved Ag^+ in the upper aqueous phase through the formation of a hydrophilic complex. The AgNPs and Ag^+ contents in the exposed cells were determined by ICP-MS after microwave digestion of the two phases, respectively. Cells treated with AgNPs at 4 °C were used as control to subtract the adhered particles.

Plasmid and transfection

Microtubule-associated protein 1 light chain 3 beta (LC3-II) fused to green fluorescent protein (GFP, Addgene Plasmid 11546) was electrically transfected using a Nucleofector™ device (Lonza, Basel, Switzerland) following the manufacturer's instructions. 2 days later, cells were exposed to the AgNPs for 24 h, and then analyzed by confocal microscopy (FV1000MPE-share, Olympus, Japan) to detect the punctuate pattern of GFP-LC3-II.

LysoTracker Red uptake assay

Ba/F3 cells were collected after the treatment of AgNPs for 24 h, and then washed twice with PBS. The cells were incubated in pre-warmed medium containing 50 nM LysoTracker Red (Life Technologies/Invitrogen, Grand Island, NY, USA) for 2 h. The cells were analyzed at 577/590 nm excitation/emission for LysoTracker Red and 350/461 nm for Hoechst 33342 by confocal microscopy and flow cytometry.

Acid phosphatase assay

The cells were collected by centrifugation after they were cultured with or without AgNPs for 24 h, and then washed and suspended with PBS before being lysed by sonication on ice. The samples were centrifuged to remove the AgNPs. The supernatant liquid containing lysosomes and lysosomal enzymes was then tested for acid phosphatase activity using an acid phosphatase assay kit (Beyotime, Shanghai, China). Finally, the absorbance at 405 nm was detected using a microplate reader (SpectraMax M5, Molecular Devices, Sunnyvale, CA, USA).

Autophagic marker dye staining

After AgNPs treatment, Ba/F3 cells were treated with 10 μM monodansylcadaverine (MDC) (Sigma) for 30 min, washed with PBS twice and analyzed by confocal microscopy.

Western blot

The cells (5×10^5 mL^{-1}) were cultured in 10 cm Petri dishes and exposed to the AgNPs at various concentrations. After treatment, the cells were washed with ice-cold PBS and lysed with 200 μL lysis buffer (Beyotime) supplemented with PMSF (final concentration 1 mM). Protein samples were separated by SDS-PAGE and transferred to an Immobilon™ PVDF membrane (Millipore, Billerica, MA, USA) using a Bio-Rad gel system (Bio-Rad, Hercules, CA, USA). The blot was performed following the instructions of the suppliers of various antibodies, including anti-LC3 (NB 100-2220, Novus Biologicals), anti-SQSTM1/p62 (#5114, Cell Signaling Technologies (CST), Danvers, MA, USA), anti-mTOR (#2983, CST) and anti-Phospho-mTOR (#2971, CST). The blot was developed with a chemiluminescence substrate (ECL) (GE Healthcare Life Sciences, Piscataway, NJ, USA) automatically (Kodak Medical X-Ray Processor 102).

Cell viability analysis

Cell viability was measured using CCK-8 assay (Cell Counting Kit-8, Beyotime) according to the manufacturer's instruction. Cells were seeded in 96-well plates (50 000 cells per 200 μL per well) and treated with AgNPs at various concentrations (0–12 μg mL^{-1}) for 24 h. Cells were then incubated with a 10 μL CCK-8 reagent for 4 h. The absorbance at two wavelengths (450 nm for a soluble dye and 650 nm for viable cells) was obtained with a microplate reader (SpectraMax M5). The relative viability of each sample was normalized to that of the untreated control cells. IC_{50} of each sample was calculated with GraphPad Prism (version 5.0).

Apoptosis assay

Annexin-V-FITC/propidium iodide (PI) labeling was performed according to the manufacturer's recommendations (Becton Dickinson). The externalization of phosphatidylserine as a marker of early-stage apoptosis was detected by the FITC-conjugated Annexin-V, whereas membrane damage due to late-stage apoptosis/necrosis was detected by the binding of PI to nuclear DNA. The apoptotic/necrotic cells were analyzed by flow cytometry. At least 10 000 cells were acquired for analysis.

DNA damage assay

After exposure to AgNPs for 24 h, the cells were washed with PBS, deposited on a slide, and then fixed in 4% formaldehyde for 10 min at room temperature. The cells were blocked in blocking buffer (1× PBS/5% normal goat serum/0.3% Triton X-100) for 60 min, and then incubated with Alexa Fluor® 488 Conjugated Phospho-Histone H2A.X rabbit mAb (CST) overnight at 4 °C. Hoechst 33342 (Sigma) was used to stain the nuclei. Prolong Gold Anti-Fade Reagent (Life Technologies) was used to mount the coverslip before the images were acquired by confocal microscopy. Lasers of 488 nm and 405 nm were used for excitation of γ-H2AX and Hoechst 33342, respectively. At least three independent experiments were conducted.

Reactive oxygen species production

To measure the intracellular generation of reactive oxygen species (ROS), the cells were loaded with a fluorescent marker 10 mM 2′,7′-dichlorodihydrofluorescein diacetate (H_2DCF-DA, Sigma) in RPMI 1640 without phenol red for 30 min, then washed with PBS, and subsequently incubated with AgNPs at various concentrations for 3 h in the dark (37 °C, 5% CO_2). The mean fluorescence intensity (MFI) was detected by flow cytometry. For each sample, the MFI of 10 000 cells was determined to represent its intracellular production of ROS.

Delivery of shRNA with a lentiviral vector

A ShRNA sequence against Atg5 was delivered to BaF3 cells with a lentiviral vector, which was purchased from Shanghai GenePharma Biotechnology with a scramble vector. The scramble and Atg5 targeted Ba/F3 cells were purified with a flow cytometer and then exposed to AgNPs for 36 h. The shRNA sequence against Atg5 was 5′-GACGTTGGTAACT-GACAAATT-3′, and the preparation of lentivirus was performed as previously described.[54] To detect the expression of Atg5, specific primers were used: forward: 5′-ATGCGGTTGAGG-CTCACTTTA-3′ and reverse: 5′-GGTTGATGGCCCAAAACTGG-3′. RNA extraction and qRT-PCR were performed as previously reported.[54]

Statistical analysis

Results were expressed as mean ± SD of at least three independent experiments. Significance was assessed by a Student's *t*-test. $*P < 0.05$ was considered as a significant difference.

Conflict of interest

The authors declare that they have no competing financial interests.

Acknowledgements

This work was supported by the grants from the National Natural Science Foundation of China (31502120), the National Natural Science Foundation of China for Key Project of International Cooperation (61420106012), the Fundamental Research Funds for the Central Universities (KJQN201620), the Natural Science Foundation of Jiangsu Province in China (BK20140716), and a Project Funded by the Priority Academic Program Development of Jiangsu Higher Education Institutions (PAPD).

Notes and references

1 H. Zazo, C. I. Colino and J. M. Lanao, Current applications of nanoparticles in infectious diseases, *J. Controlled Release*, 2016, **224**, 86–102.
2 M. Rai, A. Yadav and A. Gade, Silver nanoparticles as a new generation of antimicrobials, *Biotechnol. Adv.*, 2009, **27**, 76–83.
3 J. H. Lee, Y. S. Kim, K. S. Song, H. R. Ryu, J. H. Sung, J. D. Park, H. M. Park, N. W. Song, B. S. Shin, D. Marshak, K. Ahn, J. E. Lee and I. J. Yu, Biopersistence of silver nanoparticles in tissues from Sprague-Dawley rats, *Part. Fibre Toxicol.*, 2013, **10**, 36.
4 R. J. Vandebriel, E. C. M. Tonk, L. J. de la Fonteyne-Blankestijn, E. R. Gremmer, H. W. Verharen, L. T. van der Ven, H. van Loveren and W. H. de Jong, Immunotoxicity of silver nanoparticles in an intravenous 28-day repeated-dose toxicity study in rats, *Part. Fibre Toxicol.*, 2014, **11**, 21.
5 C. Recordati, M. De Maglie, S. Bianchessi, S. Argentiere, C. Cella, S. Mattiello, F. Cubadda, F. Aureli, M. D'Amato, A. Raggi, C. Lenardi, P. Milani and E. Scanziani, Tissue distribution and acute toxicity of silver after single intravenous administration in mice: nano-specific and size-dependent effects, *Part. Fibre Toxicol.*, 2016, **13**, 12.
6 W. H. De Jong, L. T. M. Van Der Ven, A. Sleijffers, M. V. D. Z. Park, E. H. J. M. Jansen, H. Van Loveren and R. J. Vandebriel, Systemic and immunotoxicity of silver nanoparticles in an intravenous 28 days repeated dose toxicity study in rats, *Biomaterials*, 2013, **34**, 8333–8343.
7 E. Wirawan, L. Vande Walle, K. Kersse, S. Cornelis, S. Claerhout, I. Vanoverberghe, W. Declercq, P. Agostinis, T. Vanden Berghe, S. Lippens and P. Vandenabeele, Caspase-mediated cleavage of Beclin-1 inactivates Beclin-1-induced autophagy and enhances apoptosis by promoting the release of proapoptotic factors from mitochondria, *Cell Death Dis.*, 2010, **1**, e18.
8 D. Guo, X. Zhang, Z. Huang, X. Zhou, L. Zhu, Y. Zhao and N. Gu, Comparison of cellular responses across multiple passage numbers in Ba/F3-BCR-ABL cells induced by silver nanoparticles, *Sci. China: Life Sci.*, 2012, **55**, 898–905.
9 C. A. Dos Santos, M. M. Seckler, A. P. Ingle, I. Gupta, S. Galdiero, M. Galdiero, A. Gade and M. Rai, Silver nanoparticles: therapeutical uses, toxicity, and safety issues, *J. Pharm. Sci.*, 2014, **103**, 1931–1944.
10 L. Y. Wei, J. R. Lu, H. Z. Xu, A. Patel, Z. S. Chen and G. F. Chen, Silver nanoparticles: synthesis, properties, and therapeutic applications, *Drug Discovery Today*, 2015, **20**, 595–601.
11 H. Guo, J. Zhang, M. Boudreau, J. Meng, J. Yin, J. Liu and H. Xu, Intravenous administration of silver nanoparticles causes organ toxicity through intracellular ROS-related loss of interendothelial junction, *Part. Fibre Toxicol.*, 2016, **13**, 21.
12 R. Scherz-Shouval and Z. Elazar, ROS, mitochondria and the regulation of autophagy, *Trends Cell Biol.*, 2007, **17**, 422–427.
13 N. Rubio, I. Coupienne, E. Di Valentin, I. Heirman, J. Grooten, J. Piette and P. Agostinis, Spatiotemporal autophagic degradation of oxidatively damaged organelles after photodynamic stress is amplified by mitochondrial reactive oxygen species, *Autophagy*, 2012, **8**, 312–324.
14 S. T. Stern, P. P. Adiseshaiah and R. M. Crist, Autophagy and lysosomal dysfunction as emerging mechanisms of nanomaterial toxicity, *Part. Fibre Toxicol.*, 2012, **9**, 20.
15 S. Ghavami, M. Eshragi, S. R. Ande, W. J. Chazin, T. Klonisch, A. J. Halayko, K. D. McNeill, M. Hashemi, C. Kerkhoff and M. Los, S100A8/A9 induces autophagy and apoptosis via ROS-mediated cross-talk between mitochondria and lysosomes that involves BNIP3, *Cell Res.*, 2010, **20**, 314–331.
16 Q. Zhang, W. J. Yang, N. Man, F. Zheng, Y. Y. Shen, K. J. Sun, Y. Li and L. P. Wen, Autophagy-mediated chemosensitization in cancer cells by fullerene C60 nanocrystal, *Autophagy*, 2009, **5**, 1107–1117.

17 W. Zhou, Y. Y. Miao, Y. J. Zhang, L. Liu, J. Lin, J. Y. Yang, Y. Xie and L. Wen, Induction of cyto-protective autophagy by paramontroseite VO2 nanocrystals, *Nanotechnology*, 2013, **24**, 165102.

18 T. Y. Lee, M. S. Liu, L. J. Huang, S. I. Lue, L. C. Lin, A. L. Kwan and R. C. Yang, Bioenergetic failure correlates with autophagy and apoptosis in rat liver following silver nanoparticle intraperitoneal administration, *Part. Fibre Toxicol.*, 2013, **10**, 40.

19 N. K. Verma, J. Conroy, P. E. Lyons, J. Coleman, M. P. O'Sullivan, H. Kornfeld, D. Kelleher and Y. Volkov, Autophagy induction by silver nanowires: A new aspect in the biocompatibility assessment of nanocomposite thin films, *Toxicol. Appl. Pharmacol.*, 2012, **264**, 451–461.

20 Y. Y. Xu, L. M. Wang, R. Bai, T. L. Zhang and C. Y. Chen, Silver nanoparticles impede phorbol myristate acetate-induced monocyte-macrophage differentiation and autophagy, *Nanoscale*, 2015, **7**, 16100–16109.

21 J. K. Jeong, S. Gurunathan, M. H. Kang, J. W. Han, J. Das, Y. J. Choi, D. N. Kwon, S. G. Cho, C. Park, H. G. Seo, H. Song and J. H. Kim, Hypoxia-mediated autophagic flux inhibits silver nanoparticle-triggered apoptosis in human lung cancer cells, *Sci. Rep.*, 2016, **12**, 21688.

22 A. R. Mishra, J. W. Zheng, X. Tang and P. L. Goering, Silver nanoparticle-induced autophagic-lysosomal disruption and NLRP3-inflammasome activation in HepG2 cells is size-dependent, *Toxicol. Sci.*, 2016, **150**, 473–487.

23 H. Wu, J. Lin, P. Liu, Z. Huang, P. Zhao, H. Jin, C. Wang, L. Wen and N. Gu, Is the autophagy a friend or foe in the silver nanoparticles associated radiotherapy for glioma?, *Biomaterials*, 2015, **62**, 47–57.

24 J. Lin, Z. Huang, H. Wu, W. Zhou, P. Jin, P. Wei, Y. Zhang, F. Zheng, J. Zhang, J. Xu, Y. Hu, Y. Wang, Y. Li, N. Gu and L. Wen, Inhibition of autophagy enhances the anticancer activity of silver nanoparticles, *Autophagy*, 2014, **10**, 2006–2020.

25 H. Wu, J. Lin, P. Liu, Z. Huang, P. Zhao, H. Jin, J. Ma, L. Wen and N. Gu, Reactive oxygen species acts as executor in radiation enhancement and autophagy inducing by AgNPs, *Biomaterials*, 2016, **101**, 1–9.

26 D. Guo, L. Zhu, Z. Huang, H. Zhou, Y. Ge, W. Ma, J. Wu, X. Zhang, X. Zhou, Y. Zhang, Y. Zhao and N. Gu, Anti-leukemia activity of PVP-coated silver nanoparticles via generation of reactive oxygen species and release of silver ions, *Biomaterials*, 2013, **34**, 7884–7894.

27 D. Guo, Y. Zhao, Y. Zhang, Q. Wang, Z. Huang, Q. Ding, Z. Guo, X. Zhou, L. Zhu and N. Gu, The cellular uptake and cytotoxic effect of silver nanoparticles on chronic myeloid leukemia cells, *J. Biomed. Nanotechnol.*, 2014, **10**, 669–678.

28 Y. H. Lee, F. Y. Cheng, H. W. Chiu, J. C. Tsai, C. Y. Fang, C. W. Chen and Y. J. Wang, Cytotoxicity, oxidative stress, apoptosis and the autophagic effects of silver nanoparticles in mouse embryonic fibroblasts, *Biomaterials*, 2014, **35**, 4706–4715.

29 D. Guo, J. Zhang, Z. Huang, S. Jiang and N. Gu, Colloidal silver nanoparticles improve anti-leukemic drug efficacy *via* amplification of oxidative stress, *Colloids Surf., B*, 2015, **126**, 198–203.

30 S. Schöttler, K. Klein, K. Landfester and V. Mailänder, Protein source and choice of anticoagulant decisively affect nanoparticle protein corona and cellular uptake, *Nanoscale*, 2016, **8**, 5526–5536.

31 C. Greulich, J. Diendorf, T. Simon, G. Eggeler, M. Epple and M. Koller, Uptake and intracellular distribution of silver nanoparticles in human mesenchymal stem cells, *Acta Biomater.*, 2011, **7**, 347–354.

32 A. R. Gliga, S. Skoglund, I. O. Wallinder, B. Fadeel and H. L. Karlsson, Size-dependent cytotoxicity of silver nanoparticles in human lung cells: the role of cellular uptake, agglomeration and Ag release, *Part. Fibre Toxicol.*, 2014, **11**, 11.

33 S. J. Soenen, W. J. Parak, J. Rejman and B. Manshian, (Intra)Cellular stability of inorganic nanoparticles: effects on cytotoxicity, particle functionality, and biomedical applications, *Chem. Rev.*, 2015, **115**, 2109–2135.

34 N. Mizushima, T. Yoshimori and B. Levine, Methods in mammalian autophagy research, *Cell*, 2010, **140**, 313–326.

35 Y. Kabeya, N. Mizushima, T. Uero, A. Yamamoto, T. Kirisako, T. Noda, E. Kominami, Y. Ohsumi and T. Yoshimori, LC3, a mammalian homologue of yeast Apg8p, is localized in autophagosome membranes after processing, *EMBO J.*, 2000, **19**, 5720–5728.

36 S. Barth, D. Glick and K. F. Macleod, Autophagy: assays and artifacts, *J. Pathol.*, 2010, **221**, 117–124.

37 G. Bjorkoy, T. Lamark, A. Brech, H. Outzen, M. Perander, A. Overvatn, H. Stenmark and T. Johansen, p62/SQSTM1 forms protein aggregates degraded by autophagy and has a protective effect on huntingtin-induced cell death, *J. Cell Biol.*, 2005, **171**, 603–614.

38 A. Pratsinis, P. Hervella, J. C. Leroux, S. E. Pratsinis and G. A. Sotiriou, Toxicity of silver nanoparticles in macrophages, *Small*, 2013, **9**, 2576–2584.

39 D. Guarnieri, S. Sabella, O. Muscetti, V. Belli, M. A. Malvindi, S. Fusco, E. De Luca, P. P. Pompa and P. A. Netti, Transport across the cell-membrane dictates nanoparticle fate and toxicity: a new paradigm in nanotoxicology, *Nanoscale*, 2014, **6**, 10264–10273.

40 A. Avalos, A. I. Haza, D. Mateo and P. Morales, Cytotoxicity and ROS production of manufactured silver nanoparticles of different sizes in hepatoma and leukemia cells, *J. Appl. Toxicol.*, 2014, **34**, 413–423.

41 X. Y. Yang, A. P. Gondikas, S. M. Marinakos, M. Auffan, J. Liu, H. Hsu-Kim and J. N. Meyer, Mechanism of silver nanoparticle toxicity is dependent on dissolved silver and surface coating in Caenorhabditis elegans, *Environ. Sci. Technol.*, 2012, **46**, 1119–1127.

42 M. I. Khan, A. Mohammad, G. Patil, S. A. H. Naqvi, L. K. S. Chauhan and I. Ahmad, Induction of ROS, mitochondrial damage and autophagy in lung epithelial cancer cells by iron oxide nanoparticles, *Biomaterials*, 2012, **33**, 1477–1488.

43 J. J. Li, D. Hartono, C. N. Ong, B. H. Bay and L. Y. L. Yung, Autophagy and oxidative stress associated with gold nanoparticles, *Biomaterials*, 2010, **31**, 5996–6003.
44 Y. H. Luo, S. B. Wu, Y. H. Wei, Y. C. Chen, M. H. Tsai, C. C. Ho, S. Y. Lin, C. S. Yang and P. Lin, Cadmium-based quantum dot induced autophagy formation for cell survival *via* oxidative stress, *Chem. Res. Toxicol.*, 2013, **26**, 662–673.
45 L. Hulea, Z. Markovic, I. Topisirovic, T. Simmet and V. Trajkovic, Biomedical potential of mTOR modulation by nanoparticles, *Trends Biotechnol.*, 2016, **34**, 349–353.
46 Y. B. Li, X. Zeng, S. F. Wang, Y. Sun, Z. Y. Wang, J. J. Fan, P. Song and D. Ju, Inhibition of autophagy protects against PAMAM dendrimers-induced hepatotoxicity, *Nanotoxicology*, 2015, **9**, 44–55.
47 H. L. Liu, Y. L. Zhang, N. Yang, Y. X. Zhang, X. Q. Liu, C. G. Li, Y. Zhao, Y. G. Wang, G. G. Zhang, P. Yang, F. Guo, Y. Sun and C. Y. Jiang, A functionalized single-walled carbon nanotube-induced autophagic cell death in human lung cells through Akt-TSC2-mTOR signaling, *Cell Death Dis.*, 2011, **2**, e159.
48 H. W. Chiu, T. Xia, Y. H. Lee, C. W. Chen, J. C. Tsai and Y. J. Wang, Cationic polystyrene nanospheres induce autophagic cell death through the induction of endoplasmic reticulum stress, *Nanoscale*, 2015, **7**, 736–746.
49 A. R. Solitro and J. P. MacKeigan, Leaving the lysosome behind: novel developments in autophagy inhibition, *Future Med. Chem.*, 2016, **8**, 73–86.
50 M. C. Maiuri, E. Zalckvar, A. Kimchi and G. Kroemer, Self-eating and self-killing: crosstalk between autophagy and apoptosis, *Nat. Rev. Mol. Cell Biol.*, 2007, **8**, 741–752.
51 S. Hussain, F. Al-Nsour, A. B. Rice, J. Marshburn, B. Yingling, Z. X. Ji, J. I. Zink, N. J. Walker and S. Garantziotis, Cerium dioxide nanoparticles induce apoptosis and autophagy in human peripheral blood monocytes, *ACS Nano*, 2012, **6**, 5820–5829.
52 S. Luo and D. C. Rubinsztein, Atg5 and Bcl-2 provide novel insights into the interplay between apoptosis and autophagy, *Cell Death Differ.*, 2007, **14**, 1247–1250.
53 S. Zhu, J. Zhang, L. Zhang, W. Ma, N. Man, Y. Liu, W. Zhou, J. Lin, P. Wei, P. Jin, Y. Zhang, Y. Hu, E. Gu, X. Lu, Z. Yang, X. Liu, L. Bai and L. Wen, Inhibition of Kupffer cell autophagy abrogates nanoparticle-induced liver injury, *Adv. Healthcare Mater.*, 2017, DOI: 10.1002/adhm.201601252.
54 H. Zhou, Y. Ge, L. Sun, W. J. Ma, J. Wu, X. Zhang, X. Hu, C. J. Eaves, D. Wu and Y. Zhao, Growth Arrest Specific 2 is up-regulated in chronic myeloid leukemia cells and required for their growth, *PLoS One*, 2014, **9**, e86195.

